Experimentally Delineating the Catalytic Effect of a Single Water Molecule in the Photochemical Rearrangement of the Phenylperoxy Radical to the Oxepin-2(5H)-one-5-yl Radical

Artur Mardyukov,[1] Federico J. Hernandez,[2] Lijuan Song,[1,3] Rachel Crespo-Otero,[2] and Peter R. Schreiner[1,*]

[1]Institute of Organic Chemistry, Justus Liebig University, Heinrich-Buff-Ring 17, 35392 Giessen, Germany

[2]Chemistry Department of Chemistry, University of College London, 20 Gordon Street, London, United Kingdom

[3]School of Science, Harbin Institute of Technology, Shenzhen 518055, China

KEYWORDS Catalysis, Computations, Matrix Isolation, Radicals, Transition State, Water.

ABSTRACT: Catalysis plays a pivotal role in both chemistry and biology, primarily attributed to its ability to stabilize transition states and lower activation free energies, thereby accelerating reaction rates. While computational studies have contributed valuable mechanistic insights, there remains a scarcity of experimental investigations into transition states. In this work, we embark on an experimental exploration of the catalytic energy lowering associated with transition states in the photo-rearrangement of the phenylperoxy radical-water complex to the oxepin-2(5H)-one-5-yl radical. Employing matrix isolation spectroscopy, density functional theory (DFT), and post-HF computations, we scrutinize the (photo)catalytic impact of a single water molecule on the rearrangement. Our computations indicate that the barrier heights for the water-assisted unimolecular isomerization steps are approximately 2–3 kcal mol^{-1} lower compared to the uncatalyzed steps. This decrease directly coincides with the difference in the required wavelength during the transformation ($\Delta\lambda = \lambda_{579nm} - \lambda_{546nm} \sim 3$ kcal mol^{-1})), allowing us to elucidate the transition state energy in the photochemical rearrangement of the phenylperoxy radical catalyzed by a single water molecule. Our work highlights the important role of water catalysis and has, amongst others, implications for understanding the mechanism of organic reactions under atmospheric conditions.

INTRODUCTION

Catalysis is a central theme in chemistry[1-2] and biology.[3] The general definition of catalysis is the stabilization of a transition state (TS) by lowering the activation free energy ($\Delta G^{\ddagger}$) as compared to the corresponding uncatalyzed pathway, resulting in an enhancement of the reaction rate (Scheme 1A).[4] The general fundamentals of molecular recognition of substrate and transition state typically arise from the collective action of multiple non-covalent substrate-catalyst interactions such as van der Waals[5] as well as σ-π or π-π interactions,[6-7] and hydrogen bonds[8] that may individually be weak (~0.5-5 kcal mol^{-1}) but collectively strong. Knowledge of the TS is essential for understanding the outcome of stereoselective reactions,[9] in quantum tunneling,[10-11] in the application of the Curtin-Hammett principle,[12-13] and in kinetically controlled transformations.[14] Despite the widespread use of catalytic reactions, there is scant experimental knowledge on transition states,[15-16] and most mechanistic knowledge is derived primarily from computational studies.[9, 17-19] In 2015, Field and co-workers reported a technique that allowed them to determine transition state energies from a characteristic pattern found in frequency-domain spectra of isomerization for the *cis-trans* conformational change in the S_1 state of C_2H_2 and the bond-breaking HCN-HNC isomerization.[20] Here, we present the experimental description of the transition state energy differences in the catalytic rearrangement of a phenylperoxy radical-water complex to the oxepin-2(5H)-one-5-yl radical. The catalytic effect of a single water molecule was derived by studying the photochemical rearrangement of the phenylperoxy radical–water complex using matrix isolation spectroscopy in combination with density functional theory (DFT), second-order approximate coupled-cluster (CC2), the multiconfigurational complete active space second-order perturbation (CASPT2) computations.

Given the importance of radicals in the atmosphere, the role of a water molecule as a catalyst in the oxidation of atmospheric volatile compounds has been the subject of several studies.[21] In some of the recent literature, water has been shown to drastically change the potential energy surfaces of radical-molecule reactions.[22] Water vapor is one of the most abundant atmospheric greenhouse gases. It is mainly located in the lowest layer of the atmosphere, and its concentration varies with temperature and altitude.[23-24] Water is known to form hydrogen-bonded complexes with radicals in the atmosphere, therefore affecting their absorption cross-sections and vibrational frequencies as well as their reactivity.[25-26] Even very low concentrations of these H-bonded complexes can have significant effects on atmospheric chemistry, and it is vital to comprehend the influence of water molecules on the chemical and physical properties of radicals.[25]

Scheme 1. (A) Potential energy hypersurface profiles of a catalyzed (red) vs. an uncatalyzed reaction (black). (B) Contrasting the generation and subsequent rearrangement

reactions of the phenylperoxy radical (1) with (1•H₂O, bottom) and without complexation with one water molecule.

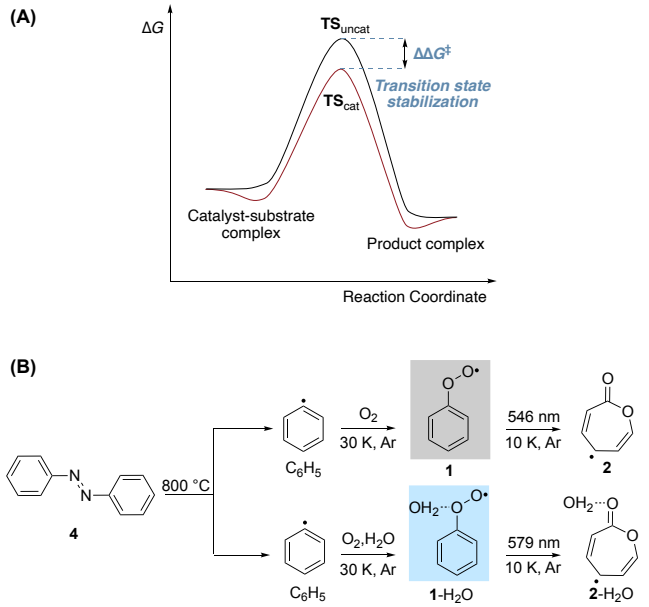

Despite their importance for atmospheric chemistry, studies on the complexes between water and radicals are scarce, because experiments are impeded by the high reactivity of radicals that requires monitoring at low temperatures[27-33] or in the gas phase.[34-37] Using finite clusters of reagent and water molecules, quantum chemical computations have suggested that the activation free energy for a variety of reactions can be significantly lowered compared to the uncomplexed case, which forms the basis for catalysis.[22, 38] Several complexes of water with •OH,[39-40] •NH₂,[41] HCO•,[42] and HOO•[35] were studied experimentally and theoretically and hydrogen bonding was found responsible for changes in reactivities. For example, the presence of water enhances the rate constant of the HOO• self-reaction.[43] The catalytic effect of a water molecule on the reaction of •OH with acetaldehyde in the gas phase was observed at low temperatures (T < 125 K).[34] According to quantum chemical computations at the CCSD(T)/cc-pVTZ level of theory, the rate enhancement is due to lowering the intrinsic reaction barrier caused by specific water aggregation.[34]

The phenyl radical (**3**) is one of the many products formed during the degradation of benzene by •OH radicals in the atmosphere.[44-45] In an oxygen-rich environment, **3** reacts with molecular oxygen (O_2) to give **1** in a barrierless process.[46] The exothermicity of this reaction ($\Delta_{rxn}H_{298}$ [$C_6H_5^\bullet + O_2 \rightarrow C_6H_5OO^\bullet$] = −46.3 kcal mol^{-1})[47-48] has been measured in both cavity ring-down[47, 49] and matrix isolation experiments.[50] However, the fate of highly reactive **1** is much less known; the decomposition of **1** is an important degradation pathway in the atmosphere. Several reaction pathways are proposed to be involved in **1** decomposition.[51] The formation of the oxepin-2(5*H*)-one-5-yl radical (**2**) was identified under matrix isolation conditions by irradiation with light λ > 450 nm and cavity-ring-down experiments.[50, 52]

Here, we present the first preparation, spectroscopic characterization, and photorearrangement of a phenylperoxy radical (**1**)–water complex (**1**•H_2O). We found that **1**•H_2O can isomerize to the oxepin-2(5*H*)-one-5-yl radical complex (**2**•H_2O) upon irradiation with light λ = 579 nm, while **1** is entirely unreactive under identical conditions: **1** isomerizes to **2** at 546 nm irradiation (Scheme 1B). This characteristic feature directly correlates with the energy of the transition state for the rate-determining step involved in this transformation. According to our computations, the corresponding barrier heights for the water-assisted unimolecular isomerization steps are approximately 2–3 kcal mol^{-1} lower compared with the uncatalyzed steps, which can directly be correlated to the energy difference of in the wavelenghts required to facilitate this transformation ($\Delta\lambda = \lambda_{579nm} - \lambda_{546nm}$). This enables us to describe the differential transition state energy in the photochemical rearrangement of the phenylperoxy radical catalyzed by a single water molecule.

RESULTS AND DISCUSSION

Following the known route for the synthesis of **1**,[53] we prepared **1** through pyrolysis (T = 800 °C) of azobenzene (**4**) in and argon matrix doped with 2% $^3O_2$ at 10 K (Scheme 1B). The oxygen adduct **1** was readily identified by its matrix IR spectrum with the strongest absorption bands at 751, 679, and 615 cm^{-1}, which nicely match with literature data (Figure S1).[50] Apart from unreacted **4**, the spectrum shows the formation of benzene as a co-product, which gives rise to characteristic absorption bands at 1040 and 675 cm^{-1} (Figure S2). The rapid thermal reaction of **1** in oxygen-doped argon matrices is usually controlled by the diffusion rate of O_2. For instance, the reactions of alkyl and aryl radicals with O_2 result in the formation of the corresponding peroxy radicals, which usually proceed without or very low barriers.[54-56] In agreement with previous work,[50] irradiation (λ = 525–546 nm) of **1** in an argon matrix at 10 K resulted in the virtually complete bleaching of the IR bands of **1** and the formation of new IR bands at 1727, 1308, 1096, and 725 and cm^{-1}, which were assigned to **2**), formed *via* a multistep rearrangement (Figure S1, Scheme 1B). Photoproduct **2** was identified by comparison with the literature[50] as well as with its computed infrared spectrum (Figure S1). Note that **1** does not rearrange to **2** upon photoexcitation (λ > 546 nm): under these conditions **1** remains photochemically inert (*vide infra*).

In argon matrices, **1** can complex a water molecule to produce **1**•H_2O. Under the matrix isolation conditions, the formation of **1**•H_2O requires that **3** first reacts with O_2 to give **1**, which then associates with H_2O to give **1**•H_2O. Both thermal steps depend on the diffusion of O_2 and H_2O, respectively. Since **3** is also photochemically highly reactive towards water, mixtures of **3**•H_2O and **1**•H_2O are expected to form when mixtures of O_2 and H_2O are used as reagents in argon.[27] To increase the yield of **1**•H_2O we therefore used an excess of O_2 compared to H_2O. When an argon matrix containing **2** doped with ca. 2% O_2 and 0.5% H_2O is slowly warmed from 10 K to 35 K the formation of **1**•H_2O as the major and **3**•H_2O as the minor product can be monitored by IR spectroscopy. Upon warming (25–35 K) the matrix all IR bands assigned to **1**•H_2O increase in intensity. Most notably, these changes occur in the area of the out-of-plane (o.o.p) C–H vibration modes between 800 and 600 cm^{-1} (Figure 1, Figure S2). New bands appeared and grew at 755, 677, and 616 cm^{-1} by increasing the water concentration and by annealing the matrix up to 35 K for several minutes (and re-cooling before measurement) (Table S1). At these temperatures, the

diffusion of matrix-isolated water becomes rapid, and the aggregation of water molecules as well as aggregates between water molecules and other trapped species takes place. In the presence of ~1% of H_2O, **1** is essentially quantitatively consumed to give **1**•H_2O. In the **1**•H_2O complex, the strong o.o.p. deformation modes of **1** at 751 and 615 cm^{-1} are blue-shifted by 4 and 1 cm^{-1}, respectively. These bands already appear at low water concentrations (0.05–0.1%), which indicates that the ratio of the complex between water and **1** is 1:1. When D_2O is used in these experiments, the o.o.p. modes of **1**•D_2O show the same shifts as with H_2O (Figure S3, Table S1). Overall, the positions and relative intensities for the experimentally observed IR bands correlate well with the computed IR bands of **1**•H_2O (Table S1). The major constituent of the photolysis products of **1**•H_2O was identified as an oxepin-2(5*H*)-one-5-yl radical complex **2**•H_2O (**2a**) (Figure 1 c-d, Figure S4).

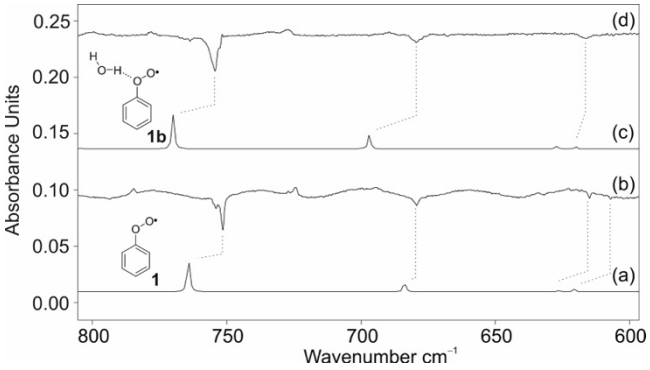

Figure 1. (a) Unscaled computed spectrum of **1** at UB3LYP-D3/6-311++G(2d,2p). (b) IR spectrum showing the product of the FVP of **4** in argon dope with 2% O_2 with subsequent trapping at 10 K. IR difference spectrum shows the changes upon 10 min 546 nm irradiation. (c) Unscaled computed spectrum for **1b** at UB3LYP-D3/6-311++G(2d,2p). (d) IR spectrum showing the product of the FVP of **4** in argon doped with 2% O_2 and 0.5% H_2O with subsequent trapping at 10 K. IR difference spectrum shows the changes upon 10 min irradiation at λ = 579 nm.

Under atmospheric conditions, the thermal formation of **2** from **1** is very unlikely because of high barriers. Instead, photochemical activation or hot ground-state reactions induced by local heating *via* internal conversion from excited states are required.[21] We examined the photochemistry of **1** and **1**–H_2O using different irradiation conditions (Figure S5). The matrix containing **1** and **1**•H_2O was first irradiated with light at λ = 525 nm for 10 s to 20 min. Irradiation at λ = 579 nm for 15 min results in the disappearance of all bands assigned to **1**•H_2O, while the bands of **1** remain unchanged. Irradiation of the matrices of **1**•H_2O with λ < 623 nm does not cause rearrangements. The IR spectrum of the new product can be assigned to a **2**•H_2O complex (Figure S3-S4). Note that **1**•H_2O rearranges to **2**•H_2O upon λ = 623 nm irradiation, though the reaction rate is slower than at λ = 576 nm (Figures S6-S7). This clearly shows a dependence of the reaction rate on the water molecule *and* the light energy. It is therefore plausible to consider a catalytic mechanism in which water modifies the potential energy surface (PES), due to the formation of H-bonded complexes between these molecules.

The structural landscape of **1**•H_2O is complicated because free **1** has multiple coordination sites. The structure, energy of complexation, and IR spectra of weakly bound complexes between **1** and H_2O were computed by using the UB3LYP-D3 and M06 functionals with a 6-311++G(2d,2p) basis set (see the Supporting Information for computational details). The water molecule stabilizes **1** through OH•••O and CH•••O hydrogen bonds (**1a** and **1b**) (Figure 2, Figure S8). Another complex between **1** and water stabilized through an OH-π interaction[57] has also been identified, but it is less stable (**1c**). Four other **1**•H_2O dimers (**1d** – **1g**) with stabilization energies between 1.9–2.1 kcal mol^{-1} were located at UB3LYP-D3/6-311++G(2d,2p). Complexes **1d** – **1g** are stabilized by CH•••O interactions between the hydrogen atom of **1** and the oxygen atom of water. Complexes **1a** and **1b** are almost isoenergetic with water binding energies of approx. 3 kcal mol^{-1}. Since the IR spectra computed for **1a** and **1b** are very similar, it was not possible to unambiguously assign which complex formed under matrix isolation conditions. The experimentally observed IR spectrum of **1**•H_2O matches well with both computed IR spectra.

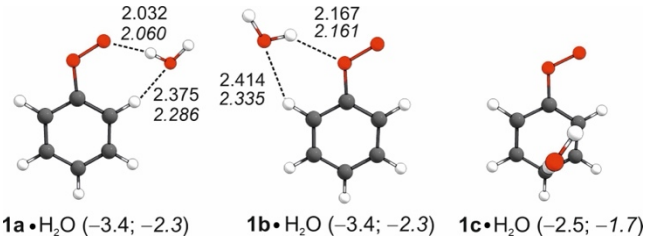

Figure 2. Computed structures with hydrogen bond lengths (Å) of **1**•H_2O complexes at UB3LYP-D3/6-311++G(2d,2p) and at UM06-2X/6-311++G(2d,2p) in italics; energies (ΔH_0, kcal mol^{-1}) with respect to the energies of separated molecules, are given in parentheses.

Furthermore, we computed the effects of water on the barriers along the isomerization pathway of **1**. As the isomerization of **1** has already been studied, we can readily compare our results for the catalyzed reaction with those from earlier uncatalyzed studies; our computations are in good agreement with previous data.[48, 51] The resulting structures and relative energies are shown in Figure 3. According to our computations, **1** isomerizes to the dioxiranyl radical **3** through COO ring closure via a barrier of 26.6 kcal mol^{-1} (**TS1**) (Figure 3). Radical **3** rearranges to triradical **4** with a barrier of 12.6 kcal mol^{-1} (**TS2**), which is the rate-determining step. Highly reactive **4** then undergoes oxygen insertion to the carbon-carbon bond *via* the barrierless **TS3** to produce **2**.

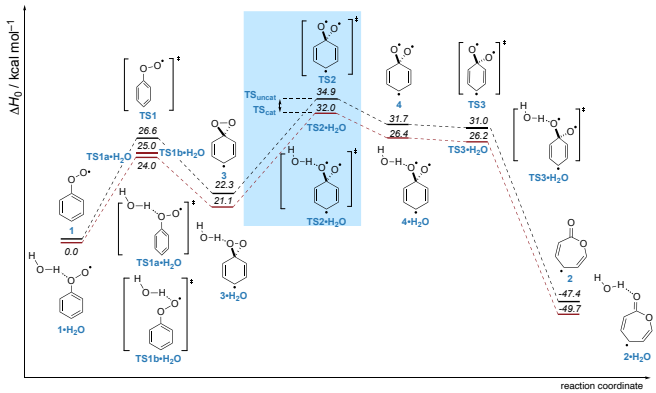

Figure 3. Potential energy profiles (ΔH_0, kcal mol^{-1}) of **1** and **1**•H_2O at UB3LYP-D3/6-311++G(2d,2p) level of theory.

The B3LYP-D3/6-311++G(2d,2p) computed isomerization paths of **1** with and without a water molecule are shown in Figure 3. The barrier height ($\Delta\Delta H^{\ddagger}$)for the water-assisted reaction in the rate determining step is 2.9 kcal mol^{-1} lower than that without a water molecule. M06-2X/6-311++G(2d,2p) gives a similar difference (2.6 kcal mol^{-1}), in overall good agreement with the experimental value of 2.9 kcal mol^{-1}, which was obtained using the energy difference of light used for water-assisted and unassisted reactions (Figure S9).

To shed light on the role of a single water molecule as a catalysts for this photochemical retransformation, we computed the vertical transitions (Tabe S1) to the first two excited states and compare their energies at the critical points of the PES (Figure 4). The S_1 state is a dark state with A" symmetry and its transition density is localized on the O–O bond (Figure 4C). The computed vertical energy for the $S_0 \rightarrow S_1$ transition (Table S2) is in excellent agreement with the value measured in jet-cooled gas phase experiments, and with the theoretically reported values, obtained at TD-B3LYP/aug-cc-PVTZ and SA4-CASPT2(15,13)/ANO-L-VDZP.[58-59] The vertical energies to S_2 are blue-shifted with respect to the experimental determinations, in line with previous computations at SA4-CASPT2(15,13)/ANO-L-VDZP level.

To understand the electronically excited-state deactivation mechanism after photo-absorption to S_2 and internal conversion to S_1, we computed the S_0 and S_1 energies of **1** and **1**•H_2O at the Franck-Condon (FC) geometry, the S_1-minimum (S_{1min}), and the closest S_1/S_0 minimum energy conical intersection (S_1/S_0-CI) geometry to S_{1min}. Complete PESs descriptions, following the mechanism depicted in Figure 3, are shown in Figure S11. The energies of a second S_1/S_0-CI geometry, close to the product geometry of **2**, its corresponding water complex **2**•H_2O, and the radical product **2** are also included. For the uncatalyzed and catalyzed cases, the MS(4)-CASPT2(11,12)/ANO-L-TZVP method suggests that the energy of S_1/S_0-CI lies below the S_{1min} value (1.4 and 3.5 kcal mol^{-1} for the uncatalyzed and catalyzed reactions, respectively) indicating that effective nonradiative deactivation to the ground state must take place. A small energy barrier from S_{1min} (2.2 kcal mol^{-1}) is computed with CC2/def2-TZVP for the uncatalyzed reaction, though. The geometry of the S_1/S_0-CI state is very similar to that of **TS1** and **TS1**•H_2O for the uncatalyzed and catalyzed reactions, respectively (Figure S12). This suggests that nonradiative excited state deactivation takes place at the early stages of the reaction, before the rate determining step (**TS2**). Therefore, water catalysis already occurs in the electronic ground state and thus before photoexcitation.

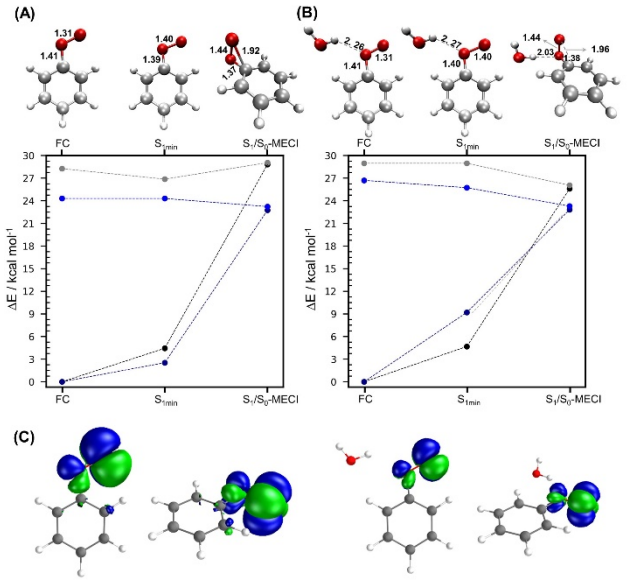

Figure 4. Energy profiles computed at MS(4)-CASPT2(11,12)/ANO-L-TZVP of the S_0 (dark blue) and S_1 (blue) states of **1** (A) and its water complexes **1**–H_2O (B). The energies computed at CC2/def2-TZVP for S_0 (black) and S_1 (gray) are also included for comparison. The geometries of the three points of the PES considered are depicted at the top of each panel along with the highlighted C-O, O-O and H…O bond distances (in Å). (C) Transition densities (top and side views) for the S_0-S_1 transition, computed at the S_{0min} geometry with SA4-CASSCF(11,12)/ANO-L-TZVP.

CONCLUSIONS

We investigated the catalytic effects associated with transition states in the rearrangement of the phenyl peroxy radical-water complex into the oxepin-2(5H)-one-5-yl radical. Employing a combination of matrix isolation IR spectroscopy, density functional theory (DFT), and multi-determinant post-HF computations, we studied the catalytic effect of a single water molecule on the rearrangement process. Our computational results reveal that the barrier heights for the water-assisted unimolecular isomerization steps are approximately 2–3 kcal mol^{-1} lower compared to the uncatalyzed steps. This decrease correlates with the difference in the required wavelength for the photochemical conversion ($\Delta\lambda = \lambda_{579nm} - \lambda_{546nm}$) of the phenylperoxy radical catalyzed by a single water molecule. Given the relevance of radicals in the atmosphere, where water is a significant component, our findings contribute to the understanding of the role association with single water molecules may play in the catalytic oxidation of volatile atmospheric compounds. Our work adds to our currently slim arsenal of experimental studies of transition states and the role of water catalysis.

ASSOCIATED CONTENT

All data are available in the main text or the supplementary information. The supplementary information includes: IR and UV/Vis spectra, IR table, Cartesian coordinates, absolute energies of all optimized geometries, experimental procedures, and computations (PDF).

AUTHOR INFORMATION

Corresponding Author

*prs@uni-giessen.de

Author Contributions

A. M. and P.R.S. conceptualized the project. A.M. collected data and wrote the original draft. P. R. S. supervised the project. A.M., F.J.H.,

L.S., and R.C.O. carried out all computations. All authors co-wrote the final manuscript.

ACKNOWLEDGMENT

This project has received funding from the European Research Council (ERC) under the European Union's Horizon 2020 research and innovation programme (Advanced Grant No. 101054751 "COLDOC" to PRS). Views and opinions expressed are those of the authors only and do not necessarily reflect those of the European Union or the European Research Council. Neither the European Union nor the granting authority can be held responsible for them. R. C. O. and F. J. H. acknowledge the funding from the Leverhulme Trust (RPG-2019-122) and the UK Materials and Molecular Model-ling Hub for computational resources, which is partially funded by EPSRC (EP/P020194/s1). L.S. also thanks the Alexander-von-Humboldt Foundation and Natural Science Foundation of Guangdong Province (2022A1515011859).

REFERENCES

1. Chan, A. Y.; Perry, I. B.; Bissonnette, N. B.; Buksh, B. F.; Edwards, G. A.; Frye, L. I.; Garry, O. L.; Lavagnino, M. N.; Li, B. X.; Liang, Y.; Mao, E.; Millet, A.; Oakley, J. V.; Reed, N. L.; Sakai, H. A.; Seath, C. P.; MacMillan, D. W. C., Metallaphotoredox: The Merger of Photoredox and Transition Metal Catalysis. *Chem. Rev.* **2022,** *122* (2), 1485-1542.

2. Cheung, K. P. S.; Sarkar, S.; Gevorgyan, V., Visible Light-Induced Transition Metal Catalysis. *Chem. Rev.* **2022,** *122* (2), 1543-1625.

3. Lerner, R. A.; Benkovic, S. J.; Schultz, P. G., At the Crossroads of Chemistry and Immunology: Catalytic Antibodies. *Science* **1991,** *252* (5006), 659-667.

4. Williams, I. H., Catalysis: transition-state molecular recognition? *Beilstein J. Org. Chem.* **2010,** (6), 1026–1034.

5. Wagner, J. P.; Schreiner, P. R., London Dispersion in Molecular Chemistry—Reconsidering Steric Effects. *Angew. Chem. Int. Ed.* **2015,** *54* (42), 12274-12296.

6. Krenske, E. H.; Houk, K. N., Aromatic Interactions as Control Elements in Stereoselective Organic Reactions. *Acc. Chem. Res.* **2013,** *46* (4), 979-989.

7. Neel, A. J.; Hilton, M. J.; Sigman, M. S.; Toste, F. D., Exploiting non-covalent π interactions for catalyst design. *Nature* **2017,** *543* (7647), 637-646.

8. Davis, H. J.; Phipps, R. J., Harnessing non-covalent interactions to exert control over regioselectivity and site-selectivity in catalytic reactions. *Chem. Sci.* **2017,** *8* (2), 864-877.

9. Sunoj, R. B., Transition State Models for Understanding the Origin of Chiral Induction in Asymmetric Catalysis. *Acc. Chem. Res.* **2016,** *49* (5), 1019-1028.

10. Schreiner, P. R.; Reisenauer, H. P.; Ley, D.; Gerbig, D.; Wu, C.-H.; Allen, W. D., Methylhydroxycarbene: Tunneling Control of a Chemical Reaction. *Science* **2011,** *332* (6035), 1300-1303.

11. Nunes, C. M.; Eckhardt, A. K.; Reva, I.; Fausto, R.; Schreiner, P. R., Competitive Nitrogen versus Carbon Tunneling. *J. Am. Chem. Soc.* **2019,** *141* (36), 14340-14348.

12. Mardyukov, A.; Quanz, H.; Schreiner, P. R., Conformer-specific hydrogen atom tunnelling in trifluoromethylhydroxycarbene. *Nat. Chem.* **2017,** *9* (1), 71-76.

13. Seeman, J. I., Effect of conformational change on reactivity in organic chemistry. Evaluations, applications, and extensions of Curtin-Hammett Winstein-Holness kinetics. *Chem. Rev.* **1983,** *83* (2), 83-134.

14. Goldstein, E.; Beno, B.; Houk, K. N., Density Functional Theory Prediction of the Relative Energies and Isotope Effects for the Concerted and Stepwise Mechanisms of the Diels−Alder Reaction of Butadiene and Ethylene. *J. Am. Chem. Soc.* **1996,** *118* (25), 6036-6043.

15. Polanyi, J. C.; Zewail, A. H., Direct Observation of the Transition State. *Acc. Chem. Res.* **1995,** *28* (3), 119-132.

16. Dantus, M.; Rosker, M. J.; Zewail, A. H., Real - time femtosecond probing of "transition states" in chemical reactions. *J. Chem. Phys.* **1987,** *87* (4), 2395-2397.

17. Allemann, C.; Gordillo, R.; Clemente, F. R.; Cheong, P. H.-Y.; Houk, K. N., Theory of Asymmetric Organocatalysis of Aldol and Related Reactions: Rationalizations and Predictions. *Acc. Chem. Res.* **2004,** *37* (8), 558-569.

18. Walden, D. M.; Ogba, O. M.; Johnston, R. C.; Cheong, P. H.-Y., Computational Insights into the Central Role of Nonbonding Interactions in Modern Covalent Organocatalysis. *Acc. Chem. Res.* **2016,** *49* (6), 1279-1291.

19. Lam, Y.-h.; Grayson, M. N.; Holland, M. C.; Simon, A.; Houk, K. N., Theory and Modeling of Asymmetric Catalytic Reactions. *Acc. Chem. Res.* **2016,** *49* (4), 750-762.

20. Baraban, J. H.; Changala, P. B.; Mellau, G. C.; Stanton, J. F.; Merer, A. J.; Field, R. W., Spectroscopic characterization of isomerization transition states. *Science* **2015,** *350* (6266), 1338-1342.

21. George, C.; Ammann, M.; D'Anna, B.; Donaldson, D. J.; Nizkorodov, S. A., Heterogeneous Photochemistry in the Atmosphere. *Chem. Rev.* **2015,** *115* (10), 4218-4258.

22. Gerber, R. B.; Varner, M. E.; Hammerich, A. D.; Riikonen, S.; Murdachaew, G.; Shemesh, D.; Finlayson-Pitts, B. J., Computational Studies of Atmospherically-Relevant Chemical Reactions in Water Clusters and on Liquid Water and Ice Surfaces. *Acc. Chem. Res.* **2015,** *48* (2), 399-406.

23. Ritchie, G., *Atmospheric Chemistry: From the Surface to the Stratosphere*. World Sci. Pub. Eu. Ltd.: 2017; p 224.

24. Brini, E.; Fennell, C. J.; Fernandez-Serra, M.; Hribar-Lee, B.; Lukšič, M.; Dill, K. A., How Water's Properties Are Encoded in Its Molecular Structure and Energies. *Chem. Rev.* **2017,** *117* (19), 12385-12414.

25. Aloisio, S.; Francisco, J. S., Radical–Water Complexes in Earth's Atmosphere. *Acc. Chem. Res.* **2000,** *33* (12), 825-830.

26. Zhong, J.; Kumar, M.; Francisco, J. S.; Zeng, X. C., Insight into Chemistry on Cloud/Aerosol Water Surfaces. *Acc. Chem. Res.* **2018,** *51* (5), 1229-1237.

27. Mardyukov, A.; Sanchez-Garcia, E.; Crespo-Otero, R.; Sander, W., Interaction and Reaction of the Phenyl Radical with Water: A Source of OH Radicals. *Angew. Chem., Int. Ed.* **2009,** *48* (26), 4804-4807.

28. Mardyukov, A.; Crespo-Otero, R.; Sanchez-Garcia, E.; Sander, W., Photochemistry and Reactivity of the Phenyl Radical-Water System: A Matrix Isolation and Computational Study. *Chem. - Eur. J.* **2010,** *16* (29), 8679-8689, S8679/1-S8679/28.

29. Costa, P.; Fernandez-Oliva, M.; Sanchez-Garcia, E.; Sander, W., The Highly Reactive Benzhydryl Cation Isolated and Stabilized in Water Ice. *J. Am. Chem. Soc.* **2014,** *136* (44), 15625-15630.

30. Plenert, A. C.; Mendez-Vega, E.; Sander, W., Micro- vs Macrosolvation in Reichardt's Dyes. *J. Am. Chem. Soc.* **2021,** *143* (33), 13156-13166.

31. Richter, G.; Mendez-Vega, E.; Sander, W., Singlet halophenylcarbenes as strong hydrogen-bond acceptors. *J. Phys. Chem. A* **2016,** *120* (20), 3524-3532.

32. Sander, W.; Roy, S.; Polyak, I.; Ramirez-Anguita, J. M.; Sanchez-Garcia, E., The Phenoxyl Radical-Water Complex-A Matrix Isolation and Computational Study. *J. Am. Chem. Soc.* **2012,** *134* (19), 8222-8230.

33. Hernandez, F. J.; Brice, J. T.; Leavitt, C. M.; Liang, T.; Raston, P. L.; Pino, G. A.; Douberly, G. E., Mid-infrared signatures of hydroxyl containing water clusters: Infrared laser Stark spectroscopy of OH–H_2O and OH(D_2O)n (n = 1-3). *J. Chem. Phys.* **2015,** *143* (16).

34. Voehringer-Martinez, E.; Hansmann, B.; Hernandez, H.; Francisco, J. S.; Troe, J.; Abel, B., Water Catalysis of a Radical-Molecule Gas-Phase Reaction. *Science* **2007,** *315* (5811), 497-501.

35. Suma, K.; Sumiyoshi, Y.; Endo, Y., The Rotational Spectrum of the Water-Hydroperoxy Radical (H_2O-HO_2) Complex. *Science* **2006,** *311* (5765), 1278-1281.

36. Leicht, D.; Kaufmann, M.; Pal, N.; Schwaab, G.; Havenith, M., From the tunneling dimer to the onset of microsolvation: Infrared spectroscopy of allyl radical water aggregates in helium nanodroplets. *J. Chem. Phys.* **2017,** *146* (11), 114306.

37. Leicht, D.; Kaufmann, M.; Schwan, R.; Schäfer, J.; Schwaab, G.; Havenith, M., Understanding the microsolvation of radicals: Infrared spectroscopy of benzyl radical water clusters. *J. Chem. Phys.* **2016,** *145* (20), 204305.

38. Jara-Toro, R. A.; Hernández, F. J.; Taccone, R. A.; Lane, S. I.; Pino, G. A., Water Catalysis of the Reaction between Methanol and OH at 294 K and the Atmospheric Implications. *Angew. Chem. Int. Ed.* **2017,** *56* (8), 2166-2170.

39. Ohshima, Y.; Sato, K.; Sumiyoshi, Y.; Endo, Y., Rotational Spectrum and Hydrogen Bonding of the H_2O–HO Radical Complex. *J. Am. Chem. Soc.* **2005,** *127* (4), 1108-1109.

40. Soloveichik, P.; O'Donnell, B. A.; Lester, M. I.; Francisco, J. S.; McCoy, A. B., Infrared Spectrum and Stability of the H_2O–HO Complex: Experiment and Theory. *J. Phys. Chem. A* **2010,** *114* (3), 1529-1538.

41. Ennis, C. P.; Lane, J. R.; Kjaergaard, H. G.; McKinley, A. J., Identification of the Water Amidogen Radical Complex. *J. Am. Chem. Soc.* **2009,** *131* (4), 1358-1359.
42. Cao, Q.; Berski, S.; Räsänen, M.; Latajka, Z.; Khriachtchev, L., Spectroscopic and Computational Characterization of the HCO···H_2O Complex. *J. Phys. Chem. A* **2013,** *117* (21), 4385-4393.
43. Kanno, N.; Tonokura, K.; Tezaki, A.; Koshi, M., Water Dependence of the HO2 Self Reaction: Kinetics of the HO_2–H_2O Complex. *J. Phys. Chem. A* **2005,** *109* (14), 3153-3158.
44. Alzueta, M. U.; Glarborg, P.; Dam-Johansen, K., Experimental and kinetic modeling study of the oxidation of benzene. *Int. J. Chem. Kinet.* **2000,** *32* (8), 498-522.
45. Atkinson, R.; Arey, J., Atmospheric Degradation of Volatile Organic Compounds. *Chem. Rev.* **2003,** *103* (12), 4605-4638.
46. Kirk, B. B.; Harman, D. G.; Kenttämaa, H. I.; Trevitt, A. J.; Blanksby, S. J., Isolation and characterization of charge-tagged phenylperoxyl radicals in the gas phase: direct evidence for products and pathways in low temperature benzene oxidation. *Phys. Chem. Chem. Phys.* **2012,** *14* (48), 16719-16730.
47. Yu, T.; Lin, M. C., Kinetics of the C_6H_5 + O_2 Reaction at Low Temperatures. *J. Aa. Chem. Soc.* **1994,** *116* (21), 9571-9576.
48. Tokmakov, I. V.; Kim, G.-S.; Kislov, V. V.; Mebel, A. M.; Lin, M. C., The Reaction of Phenyl Radical with Molecular Oxygen: A G2M Study of the Potential Energy Surface. *J. Phys. Chem. A* **2005,** *109* (27), 6114-6127.
49. Just, G. M. P.; Sharp, E. N.; Zalyubovsky, S. J.; Miller, T. A., Cavity ringdown spectroscopy of the $A^{\sim}$–$X^{\sim}$ electronic transition of the phenyl peroxy radical. *Chem. Phys. Lett.* **2006,** *417* (4), 378-382.
50. Mardyukov, A.; Sander, W., Matrix isolation and spectroscopic characterization of the phenylperoxy radical and its rearranged products. *Chem. - Eur. J.* **2009,** *15* (6), 1462-1467.
51. Morozov, A. N.; Medvedkov, I. A.; Azyazov, V. N.; Mebel, A. M., Theoretical Study of the Phenoxy Radical Recombination with the O(^{3}P) Atom, Phenyl plus Molecular Oxygen Revisited. *J. Phys. Chem. A* **2021,** *125* (18), 3965-3977.
52. Tanaka, K.; Ando, M.; Sakamoto, Y.; Tonokura, K., Pressure dependence of phenylperoxy radical formation in the reaction of phenyl radical with molecular oxygen. *Int. J. Chem. Kinet.* **2012,** *44* (1), 41-50.
53. Menez, B.; Pisapia, C.; Pisapia, C.; Jamme, F.; Dumas, P.; Refregiers, M.; Andreani, M.; Vanbellingen, Q. P.; Brunelle, A.; Richard, L., Abiotic synthesis of amino acids in the recesses of the oceanic lithosphere. *Nature* **2018,** *564* (7734), 59-63.
54. Mardyukov, A.; Schreiner, P. R., Generation and characterization of the phenylthiyl radical and its oxidation to the phenylthiylperoxy and phenylsulfonyl radicals. *Phys. Chem. Chem. Phys.* **2016,** *18* (37), 26161-26165.
55. Mardyukov, A.; Tsegaw, Y. A.; Sander, W.; Schreiner, P. R., The phenylselenyl radical and its reaction with molecular oxygen. *Phys. Chem. Chem. Phys.* **2017,** *19* (40), 27384-27388.
56. Keul, F.; Mardyukov, A., Generation and reactivity of vinyltelluryl radical. *Phys. Chem. Chem. Phys.* **2022,** *24* (24), 15129-15134.
57. Medel, R.; Heger, M.; Suhm, M. A., Molecular Docking via Olefinic OH···π Interactions: A Bulky Alkene Model System and Its Cooperativity. *J. Phys. Chem. A* **2015,** *119* (9), 1723-1730.
58. Freel, K. A.; Sullivan, M. N.; Park, J.; Lin, M. C.; Heaven, M. C., Structure in the Visible Absorption Bands of Jet-Cooled Phenylperoxy Radicals. *J. Phys. Chem. A* **2013,** *117* (32), 7484-7491.
59. He, X.; Zhao, Z.-X.; Zhang, H.-X., Further studies into the photodissociation pathways of phenylperoxyl radicals. *Comput. Theor. Chem.* **2015,** *1068*, 104-108.

TOC graphics: